Supporting information

DNA-Mediated Peptide Assembly into Protein Mimics

Fangzhou Zhao[a], Martin Frandsen[b], Sabrina Capodaglio[c], and Hanadi F. Sleiman[a]*

[a]Department of Chemistry, McGill University, 801 Sherbrooke St. W., Montreal, QC, H3A0B8, Canada

[b]Department of Chemistry and Interdisciplinary Nanoscience Centre (iNANO), Aarhus University, Gustav Wieds Vej 14, 8000 Aarhus C, Denmark

[c]Department of Chemistry, Life Sciences and Environmental Sustainability, University of Parma, Parco Area delle Scienze 17/A, I-43124 Parma, Italy

*E-mail: hanadi.sleiman@mcgill.ca

Table of Contents

I. Materials

SigmaAldrich supplied acetic acid, sodium chloride, sodium fluoride, dimethyl sulfoxide (DMSO), acetonitrile (ACN), triethylamine (TEA), tris(3hydroxypropyltriazolylmethyl) amine (THPTA), copper (II) sulphate (CuSO4), magnesium chloride hexahydrate, N,N'-dicycolhexylcarbodiimide, and bromoacetic acid N-hydroxysuccinimide ester. LGC Biosearch and Chemgenes supplied 1 μmol Universal 1000Å LCAA-CPG solid supports and automated DNA synthesis reagents. BioShop supplied EDTA, acrylamide (40%)/bisacrylamide 19:1 solution, urea, tris, tetramethylenediamine, and ammonium persulfate. VWR provided GelRed™. Sigma supplied Rink Amide resin (100-200 mesh) and peptide synthesis reagents. Oakwood supplied 5-hexynoic acid for modification on peptide N-terminus. Amicon 3k was purchased from Sigma, which was employed to desalt the sample before HPLC purification. GeneRuler Ultra Low Range DNA ladder was purchased from Thermofisher. IDT supplied all the linear DNA strands. 3-heptad peptides (P1, P2 and P3) were ordered from Biomatik. 1xTAMg buffer contains 45 mM Tris and 12.5 mM $MgCl_2$•$6H_2O$ with a pH of 8.0 adjusted with glacial acetic acid. The composition of 1xTBE buffer is 90 mM Tris, 90 mM boric acid, and 2 mM EDTA with a pH of 8.3. The mobile phase of TEAA is 50 mM triethylammonium acetate with a pH of 8.0 that has been adjusted with glacial acetic acid.

II. Instrumentation

The branching DNA trimers were generated using standard automated solid-phase oligonucleotide synthesis on a 1 μmol scale using a BioAutomation MerMade MM6 DNA synthesizer. To purify crude materials, polyacrylamide gel electrophoresis (PAGE) was utilised (20 x 20 cm vertical Hoefer 600 electrophoresis equipment). Using Bio-Rad Laboratories' ChemiDocTM MP System, gel images were collected. Using a NanoDrop Lite Spectrophotometer and molar extinction coefficients, DNA quantification was accomplished at 260 nm and peptide quantification was accomplished at 280 nm. Single stranded and branching DNA-peptide conjugates were purified by Agilent 1260 Infinity HPLC (high performance liquid chromatography) system equipped with a Hamilton PRP-1 RP (reverse phase) column. Using an Eppendorf Mastercycler® 96 well thermocycler, DNA nanostructures were subjected to thermal annealing. Using a Dionex Ultimate 3000 linked to a Bruker MaXis Impact™ QTOF, LC-ESI-MS was performed. Circular Dichroism (CD) was performed on JASCO J-810 spectropolarimeter equipped with a xenon lamp in a 1 mm path length quartz cuvette. Thermal melting experiments were accomplished in Cary UV-Vis Multicell Peltier, Chirascan circular dichoism instrument and JASCO J-810 spectropolarimeter.

III. DNA sequences

Description	Name	Sequences (5'-3')
Amine modified DNA	sAT'	/5AmMC6/TCAGTTGACCATATA
	sDT'	/5AmMC6/TATGGACCAAGGCCA
	sHT'	/5AmMC6/TGCCAGTATAGAAGA
3-way junction (3WJ scaffold strands)	W1AB	AAATCTCGAACACA TTTATATGGTCAACTGAAAAA AAAAAGTAATACCAGATGGTT CTAGTCGGCACTTC

		W2HE	TTAACCGGCGGCCT TTTCTTCTATACTGGCAAAAA AAAAACAGGATTAGCAGAGTT ACAACCAATGGCTT
		W3DI	AGATAGTGTACCGC TTTGGCCTTGGTCCATAAAAA AAAAAACCGCGACTGCGAGTT TGCGCCACACCGTA
		D1	GAAGTGCCGACTAG AGGCCGCCGGTTAA
		D2	AAGCCATTGGTTGT GCGGTACACTATCT
		D3	TACGGTGTGGCGCA TGTGTTCGAGATTT
		TB	CCATCTGGTATTACTTTTT
		TE	TCTGCTAATCCTGTTTTT
		TI	CGCAGTCGCGGTTTTTT
Stretching scaffolds	Spacer = 15 bp	A15	TGGCCTTGGTCCATAAACCTATCTTCGCGG
		D15	TATATGGTCAACTGACCGCGAAGATAGGTT
	Spacer = 25 bp	A25	TGGCCTTGGTCCATAGATCGCCACTAACCTATCTTCGCGG
		D25	TATATGGTCAACTGACCGCGAAGATAGGTTAGTGGCGATC

Table S1. Linear DNA sequences used in this study.

IV. Synthesis of DNA scaffold trimer

DNA scaffold trimer was synthesized via solid phase phosphoramidite oligo synthesis. Reverse phosphoramidites (3'-DMT 5'-CED) were used for first branch synthesis so that it proceeded from 5' to 3'. Afterwards, asymmetrical branching CED phosphoramidite was conjugated to the DNA chain, and the second branch synthesis proceeded from 3' to 5' after DMT removal. The second arm's 5' end was treated with CAP solution and the levulinyl protecting group was removed by 0.5M hydrazine hydrate in 1:1 pyridine/acetic acid for 10 mins permitting the third arm synthesis using normal phosphoramidite. The strand was cleaved from the CPG in ammonium hydroxide and purified by a denaturing PAGE gel.

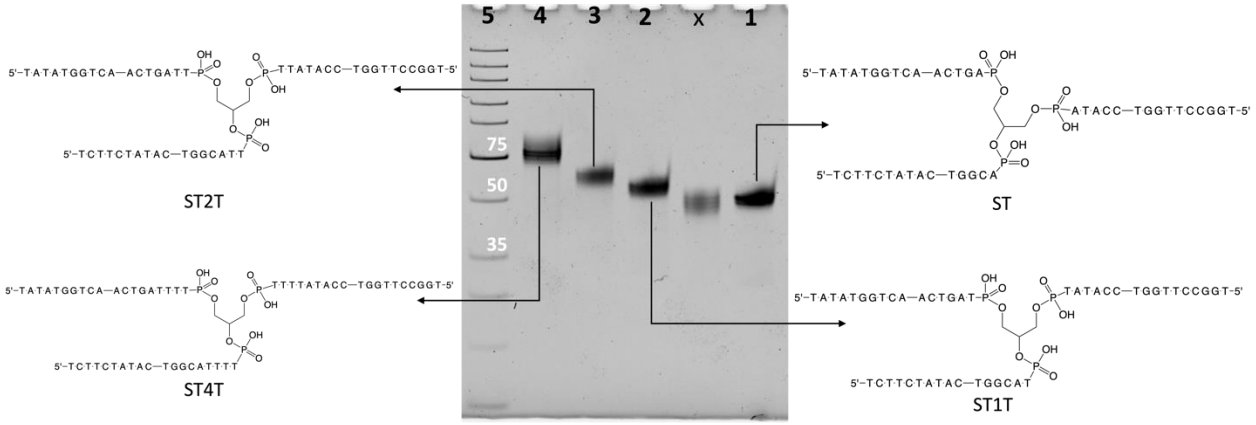

Figure S1. Denaturing gel of purified scaffolds. Lane 1: scaffold trimer (ST), 2: scaffold trimer with 1 T central spacer (ST1T), 3: scaffold trimer with 2 T central spacer (ST2T), 4: scaffold trimer with 4 T central spacer (ST4T), 5: ultra-low range ladder. Lane x indicates the lane which is not related to this study.

V. Manual solid phase peptide synthesis

All 2-heaptd peptides (P4-P11) were produced by solid phase peptide synthesis manually. Anhydrous DMF were stored in molecular sieves and degassed for 30 mins with Argon before use. H-Rink amide resin was allowed to swell in DCM for 30-60mins prior to the synthesis. The first amino acid Fmoc-Cys-OH (5 eq.), DIC (10 eq.) and HOBt hydrate (10 eq.) were premixed in DMF and then incubated with the resin for 4 hours to allow for the loading. The liquid is then removed by suction and resin was washed by DMF and DCM. The obtained resin was then treated with 20% pipiridine in DMF (2*8 mins) to remove the Fmoc protecting group. Followed by DCM and dry DMF wash, a solution of the second Fmoc-AA-OH (5 eq.), HBTU (4.5 eq.) and DIPEA (10 eq.) premixed for 2 mins in anhydrous DMF was delivered to the resin and incubated for 30 mins. The resin was then washed by DMF and DCM again after the coupling reaction. This cycle was repeated until the desired peptide sequence is achieved. 5-hexynoic acid is used as the last coupling unit. The resin bearing full peptide sequence was treated with 0.5 mL cocktail consisting of TFA:H_2O:Ethaneditiol:TIPS (94:2.5:2.5:1) for 1 hour twice to allow for the cleaving. The acquired peptide-containing solution was mixed with 50 mL Et_2O and stored at -20 °C overnight. Peptide solid was collected after centrifugation and supernatant removal. The obtained flake was dried under vacuum and characterized by ESI-MS (**Figure S2**).

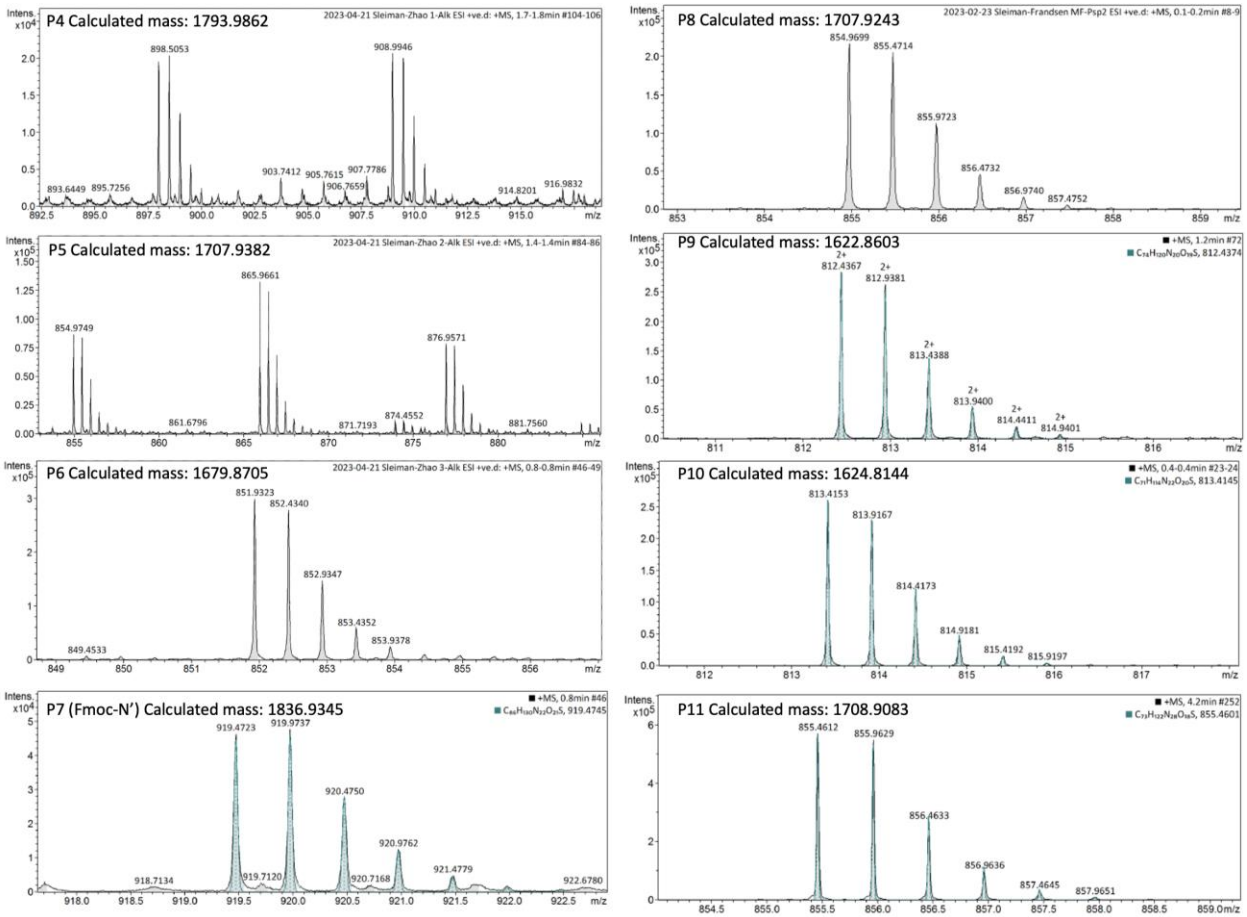

Figure S2. MS characterization of 2-heptad peptides**.**

VI. Synthesis of DNA-peptide conjugates and stapling

1. Synthesis of single stranded DNA-peptide conjugates

Amino modified oligo (15 nmol, 7.5 µL, 2 mM) and borate buffer (0.1M, pH = 8.5, 15 µL) is added to a solution of bromoacetic acid N-hydroxysuccinimide ester (0.5 mg, 15 µL, DMSO). The reaction mixture is incubated at RT in the dark for 1 hour and is then diluted to 100 µL with MQ. The mixture is then ethanol precipitated (250 µL 96% EtOH, 14 µL 3M NaOAc, 1 µL Glucogen (20 mg/mL)), snap frozen in liquid nitrogen followed by centrifugation for 1 h (10 °C, 13000 RPM). Immediately hereafter, a solution of peptide (37.5 nmol, 37.5 µL, 1 mM) in PBS (100 uL) is added to dissolve the pellet and the mixture is incubated at 37 °C overnight. The sample is then purified by RP-HPLC (**Figure S3**) and product containing fractions are lyophilized. The ethanol DNA precipitation step recovered 60-80% of the DNA in solution after formation of the bromoacetamide. The HPLC chromatograph indicated a conversion yield of 40-50% for single stranded DNA-peptide conjugates. The overall isolation yield varied from 20-33%. HPLC method is as follow: 0-2 mins: TEAA/ACN = 97/3; 2-32 mins: TEAA/ACN from 97/3 to 50/50. All single stranded DNA-peptide conjugates were characterized by ESI-MS (**Figure S4**).

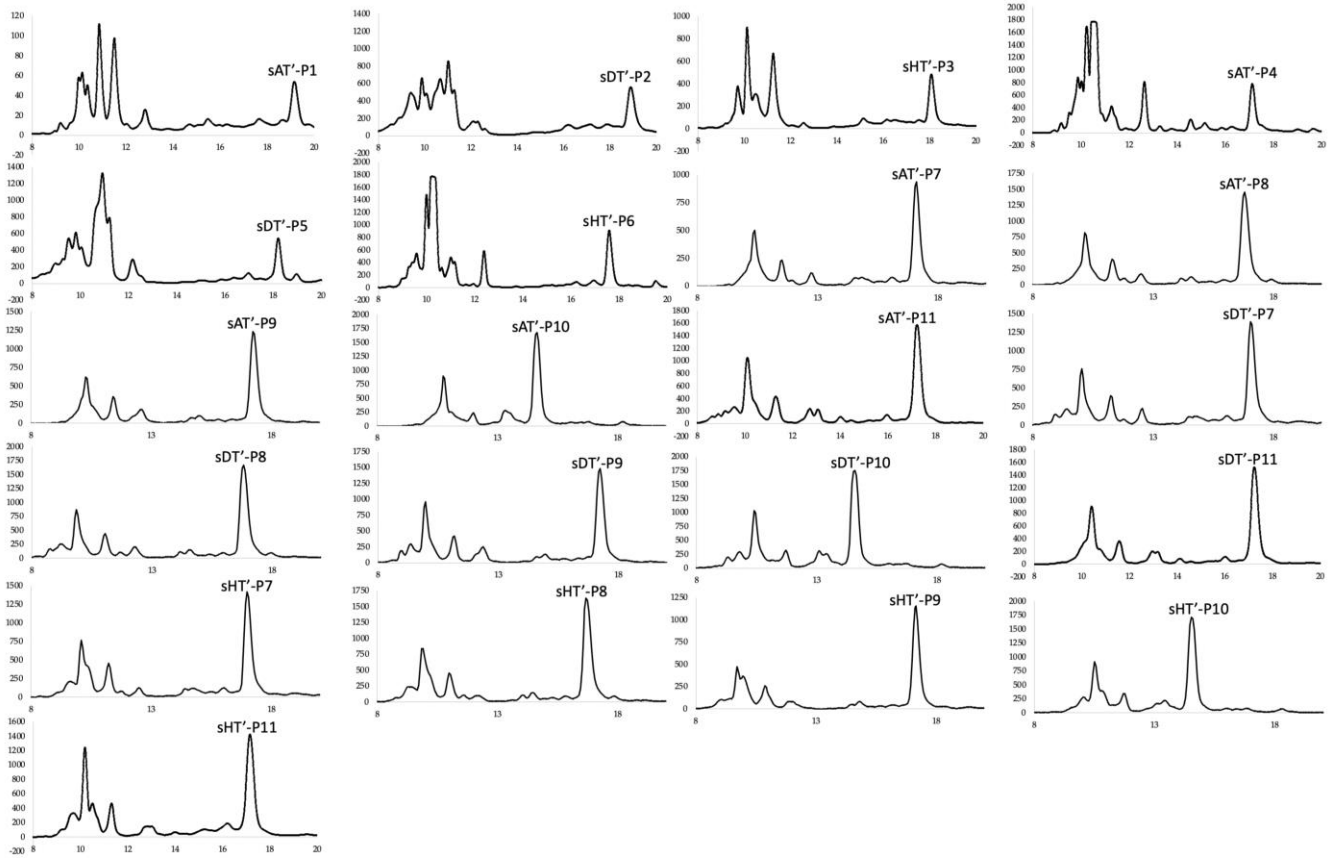

Figure S3. RP-HPLC chromatograph of single stranded DNA-peptide conjugates (I, **Figure 1b**). X axis: time/mins; Y axis: A260/mAU.

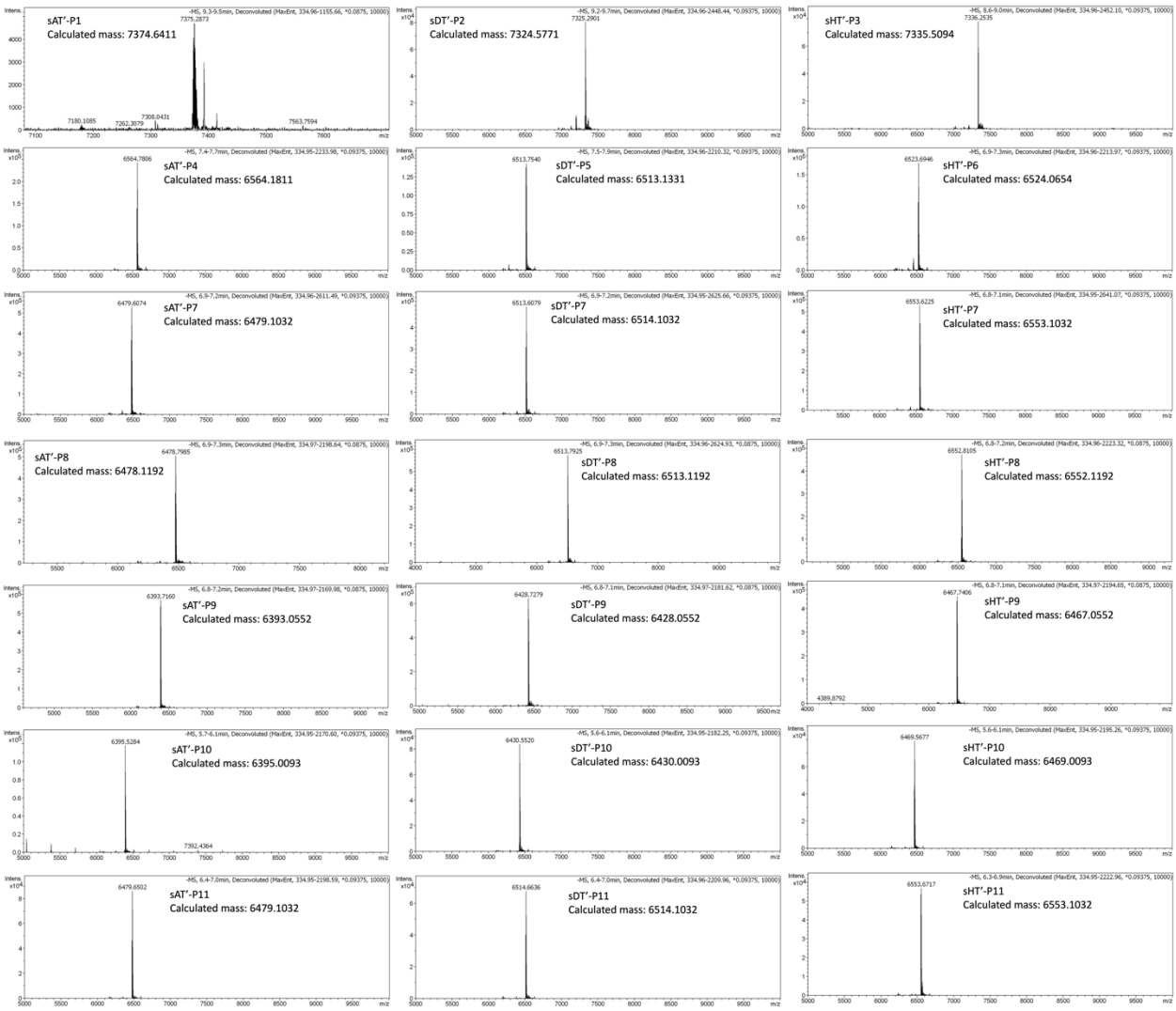

Figure S4. MS characterization of single stranded DNA-peptide conjugates (I, **Figure 1b**).

2. Stapling of single stranded conjugates into branching DNA-peptide trimer

DNA scaffold, sAT'-peptide, sDT'-peptide, and sHT'-peptide were mixed 10/10/10/10 μM in 1x PBS and incubated at RT for 1hr prior to the stapling reaction. $CuSO_4$ (2 mM), THPTA (5 mM), 1,3,5-tris(azidomethyl)benzene (25 μM), and sodium ascorbate (12 mM) were added to a separate Eppendorf tube sequentially and incubated in 1x PBS/DMSO = 4/1 at RT for 15 mins. The mixture was added to the DNA solution afterwards and the final concentration is as follow: DNA assembly (5 μM), CuSO4 (1 mM), THPTA (2.5 mM), 1,3,5-tris(azidomethyl)benzene (12.5 μM), sodium ascorbate (6mM), DMSO (10% volume). The reaction solution was incubated at 37 °C for 1 hour. Followed by the addition of 1 volume 8 M urea aqueous solution, the denatured crude was concentrated by Amikon® Ultra-0.5mL Centrifugal Filter 3 kDa MWCO Millipore (30 min, 13.000 RPM) and washed with 4 M urea twice and Milli-Q water twice in the same filter. The desalted sample was then purified by RP-HPLC (**Figure S6**). HPLC method is as follow: 0-2 mins: TEAA/ACN = 97/3; 2-5 mins: TEAA/ACN from 97/3 to 85/15; 5-32 mins: TEAA/ACN from 85/15 to 75/25; 32-35 mins: TEAA/ACN = 75/25. Branching DNA-peptide trimer product containing fractions were lyophilized and characterized by ESI-MS.

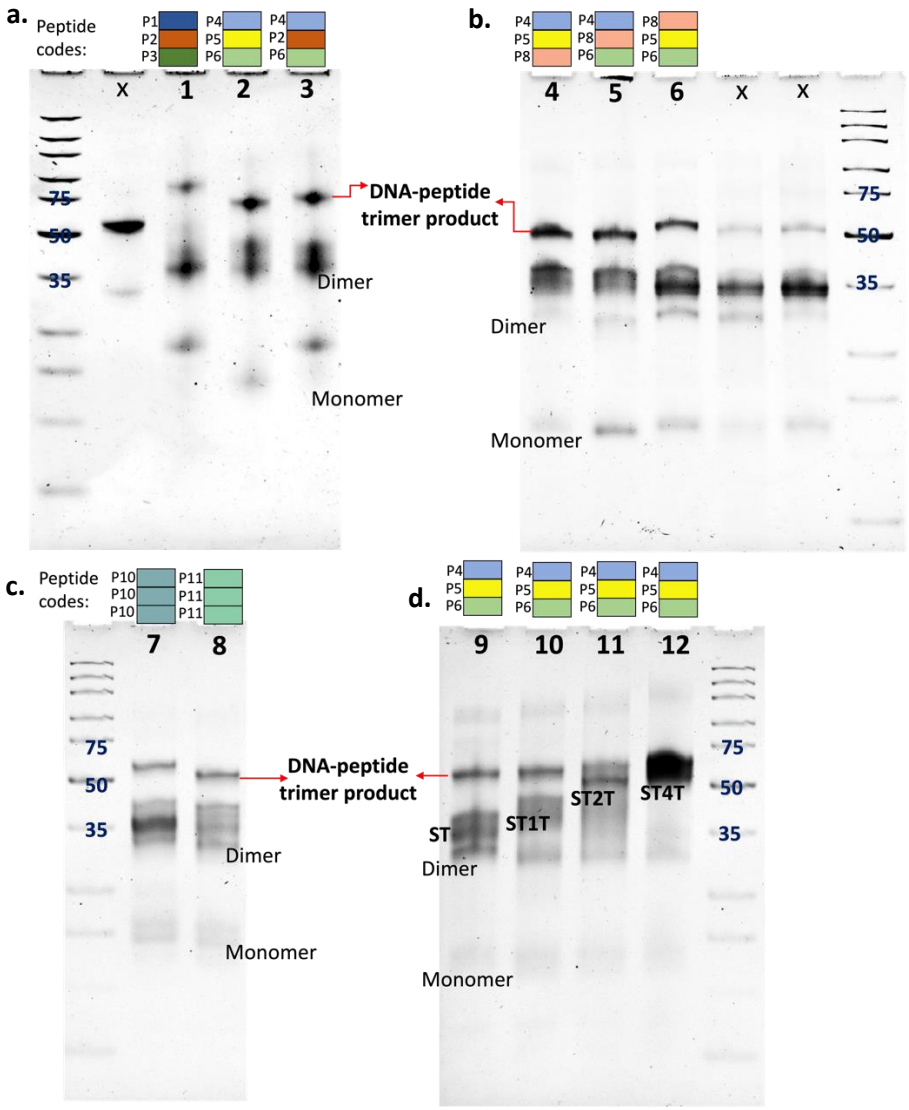

Figure S5. Denaturing gel of stapling reaction crudes. Ultra-low range DNA ladder was used in all gels. **a**) Branching DNA-peptide trimer with different peptide lengths. Lane 1: Trimer comprising three 3-heptad peptides, 2: three 2-heptad peptides, 3: two 2-heptad peptides and one 3-heptad peptide. **b**) DNA-peptide trimer with peptide conjugating to DNA at different positions, and weak peptide-peptide interactions. Lane 4-6: Trimer comprising two peptides conjugating to DNA at **f** position, and one peptide conjugating to DNA at **a** position. Repulsive interhelical ion pairs were present in the peptide combinations. **c**) DNA-peptide trimer with week peptide-peptide interactions. Lane 7: peptide combinations in lack of hydrophobic core, 8: with repulsive ion pairs. **d**) DNA-peptide trimer E2 stapled on scaffolds with different central spacers. A similar conversion yield was observed on each scaffold-templated reaction. Lane 9: stapling reaction templated by scaffold trimer (ST), 10: scaffold trimer – 1 T (ST1T), 11: scaffold trimer – 2 T (ST2T), 12: scaffold trimer – 4 T (ST4T). Lane x indicates the lanes which are not related to this study.

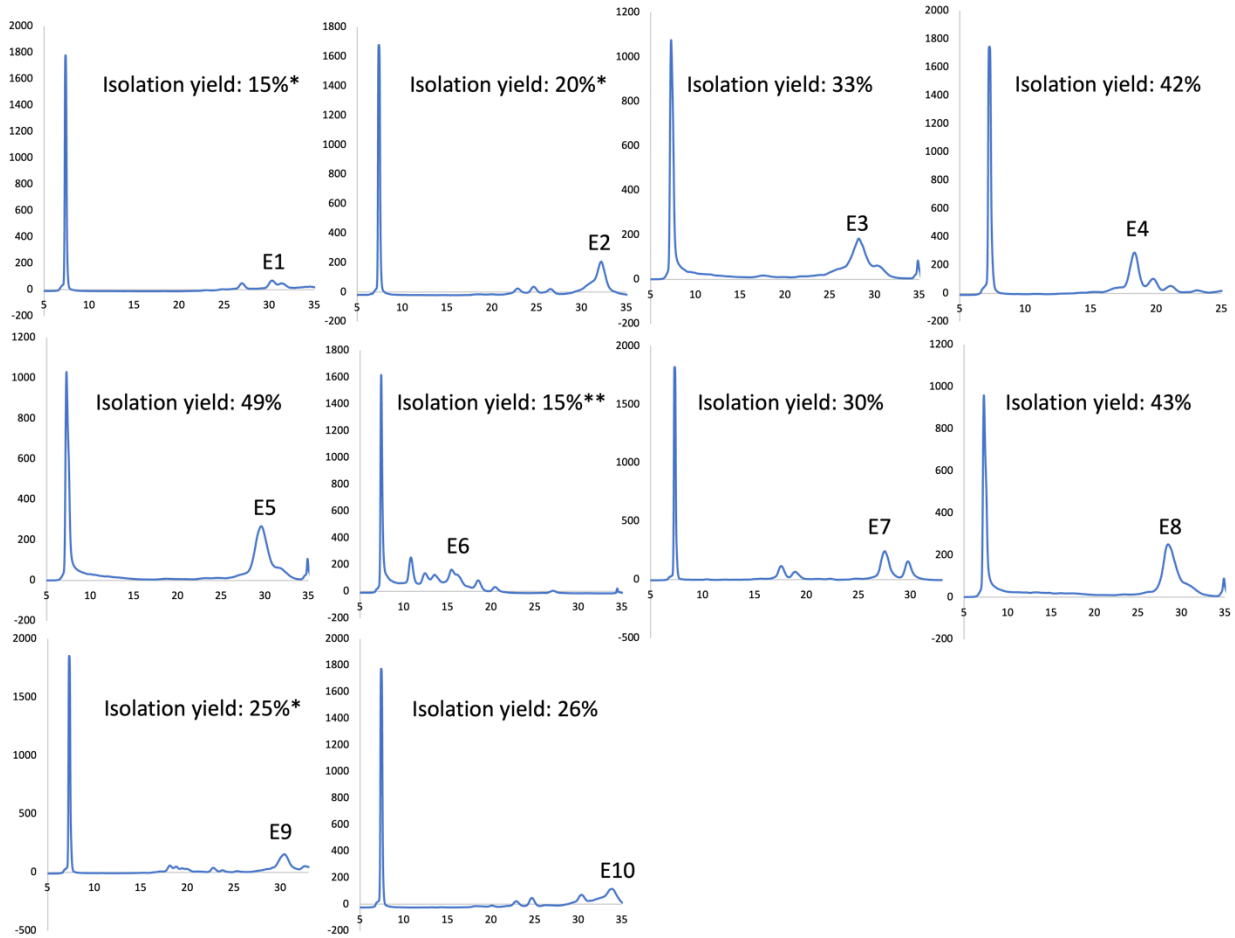

Figure S6. Isolation yield and preparative RP-HPLC chromatograph of stapled protein mimics (IV, **Figure 1b**) in **Table 2**. X axis: time/mins; Y axis: A260/mAU. * indicates that DNA-peptide got lost during the Amicon 3K desalting step prior to HPLC injection; ** indicates that DNA-peptide trimer got lost during HPLC separation.

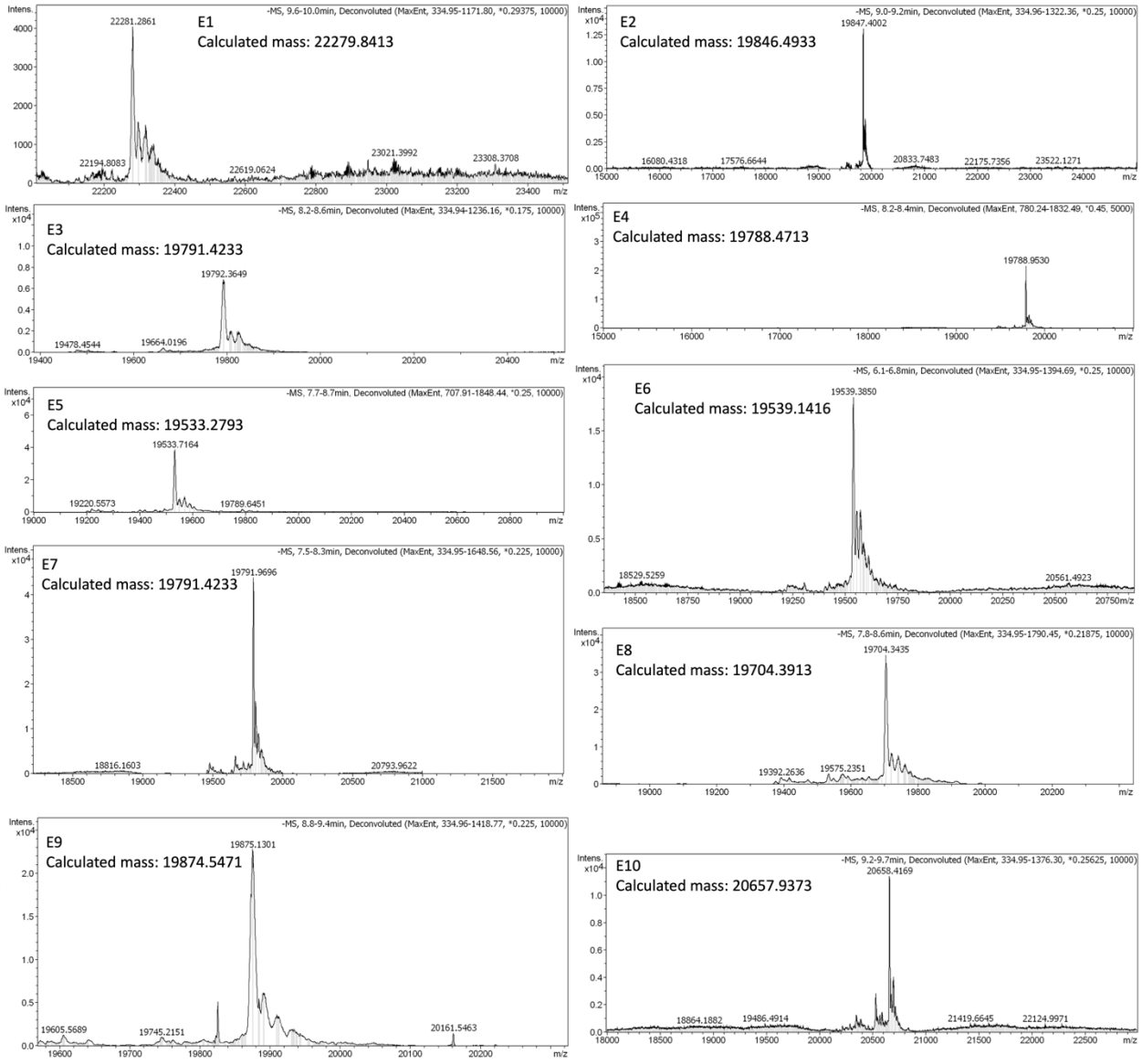

Figure S7. MS characterization of stapled protein mimics (IV, **Figure 1b**) in **Table 2**.

VII. DNA assembly and CD experiment

1. DNA nanostructure's assembly

All structures were assembled in 1x NaF buffer (pH = 7.4) containing 138.2 mM NaF, 10mM Na_2HPO_4 and 1.8 mM NaH_2PO_4 to get a clean background in short wavelength region on CD spectrum. Assembly protocols is as follow: *a.* 30 mins at RT; *b.* 95 to 4 °C in 60 mins; Sample preparation procedures were given in the table below (**Table S2**).

Entry	Structure	Component	Assembly protocol

1 n=63	ss DP	5 µM of sAT'-P1, sDT'-P2, sHT'-P3	*a.*
	ds DP	5 µM of sAT'-P1, sDT'-P2, sHT'-P3, ST	*a.*
	ss Trimer	1 µM of branching trimer E1	*a.*
	ds Trimer	1 µM of branching trimer E1, ST	*b.*
2 n=42	ss DP	5 µM of sAT'-P4, sDT'-P5, sHT'-P6	*a.*
	ds DP	5 µM of sAT'-P4, sDT'-P5, sHT'-P6, ST	*a.*
	ss Trimer	4 µM of branching trimer E2	*a.*
	ds Trimer	3.2 µM of branching trimer E2, ST	*b.*
3 n=39	ss DP	5 µM of sAT'-P7, sDT'-P7, sHT'-P7	*a.*
	ds DP	5 µM of sAT'-P7, sDT'-P7, sHT'-P7, ST	*a.*
	ss Trimer	5 µM of branching trimer E3	*a.*
	ds Trimer	5 µM of branching trimer E3, ST	*b.*
4 n=39	ss DP	5 µM of sAT'-P8, sDT'-P8, sHT'-P8	*a.*
	ds DP	5 µM of sAT'-P8, sDT'-P8, sHT'-P8, ST	*a.*
	ss Trimer	5 µM of branching trimer E4	*a.*
	ds Trimer	5 µM of branching trimer E4, ST	*b.*
5 n=39	ss DP	5 µM of sAT'-P9, sDT'-P9, sHT'-P9	*a.*
	ds DP	5 µM of sAT'-P9, sDT'-P9, sHT'-P9, ST	*a.*
	ss Trimer	5 µM of branching trimer E5	*a.*
	ds Trimer	5 µM of branching trimer E5, ST	*b.*
6 n=39	ss DP	5 µM of sAT'-P10, sDT'-P10, sHT'-P10	*a.*
	ds DP	5 µM of sAT'-P10, sDT'-P10, sHT'-P10, ST	*a.*
	ss Trimer	3 µM of branching trimer E6	*a.*
	ds Trimer	3 µM of branching trimer E6, ST	*b.*
7 n=39	ss DP	5 µM of sAT'-P11, sDT'-P11, sHT'-P11	*a.*
	ds DP	5 µM of sAT'-P11, sDT'-P11, sHT'-P11, ST	*a.*
	ss Trimer	3 µM of branching trimer E7	*a.*
	ds Trimer	3 µM of branching trimer E7, ST	*b.*
	ss DP	5 µM of sAT'-P7, sDT'-P8, sHT'-P9	*a.*

8 n=39	ds DP	5 μM of sAT'-P7, sDT'-P8, sHT'-P9, ST	*a.*
	ss Trimer	5 μM of branching trimer E8	*a.*
	ds Trimer	5 μM of branching trimer E8, ST	*b.*
9 n=41	ss DP	5 μM of sAT'-P4, sDT'-P5, sHT'-P8	*a.*
	ds DP	5 μM of sAT'-P4, sDT'-P5, sHT'-P8, ST	*a.*
	ss Trimer	5 μM of branching trimer E9	*a.*
	ds Trimer	5 μM of branching trimer E9, ST	*b.*
10 n=49	ss DP	5 μM of sAT'-P4, sDT'-P2, sHT'-P6	*a.*
	ds DP	5 μM of sAT'-P4, sDT'-P2, sHT'-P6, ST	*a.*
	ss Trimer	2.6 μM of branching trimer E10	*a.*
	ds Trimer	2.6 μM of branching trimer E10, ST	*b.*

Table S2. Sample preparation procedures. n = number of amino acids used for mean residue molar ellipticity calculation (**SI VII-3**).

2. CD characterization of peptide

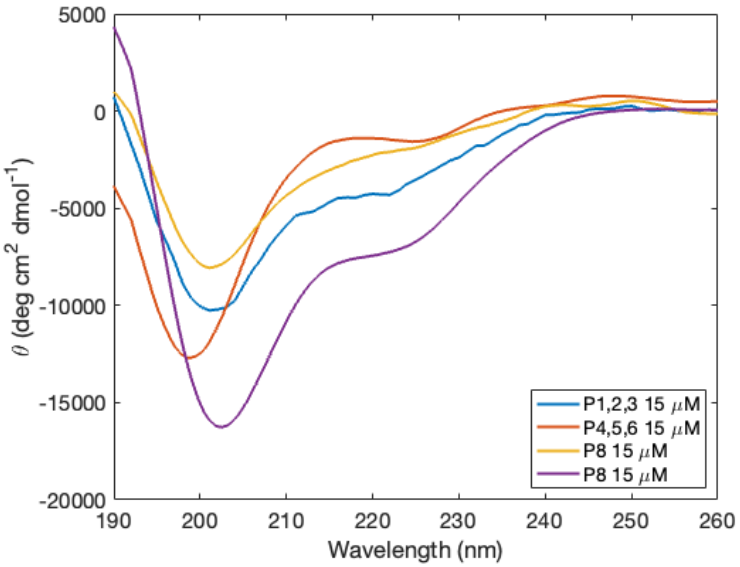

Figure S8. Spectra of peptide samples. Blue: solution mixture of P1, P2 and P3 (1:1:1), total peptide concentration is 15 μM; Orange: solution mixture of P4, P5 and P6 (1:1:1), total peptide concentration is 15 μM; Yellow: solution of P8, total peptide concentration is 15 μM; Purple: solution of P8, total peptide concentration is 50 μM.

3. CD characterization of DNA-peptide conjugates

The assembled structures were loaded in a 1mm quartz cuvette and characterized in JASCO J810 circular dichroism instrument at 20 °C. Sensitivity was set at Standard, D.I.T. was 4 sec, Bandwidth was 2.00 nm, and scanning speed was 100 nm/min for all cases. To compare the CD spectra of different constructs, mean residue molar ellipticity was calculated using the following equation:

$$\theta(deg \cdot cm^2 \cdot dmol^{-1}) = \frac{Ellipticity(mdeg) \times 10^5}{l \times c \times n}$$

where *Ellipticity* is the raw output from the instrument, *l*(cm) is the pathlength, *c*(μM) is the nanostructure's concentration and *n* is the number of amino acids in each structure.

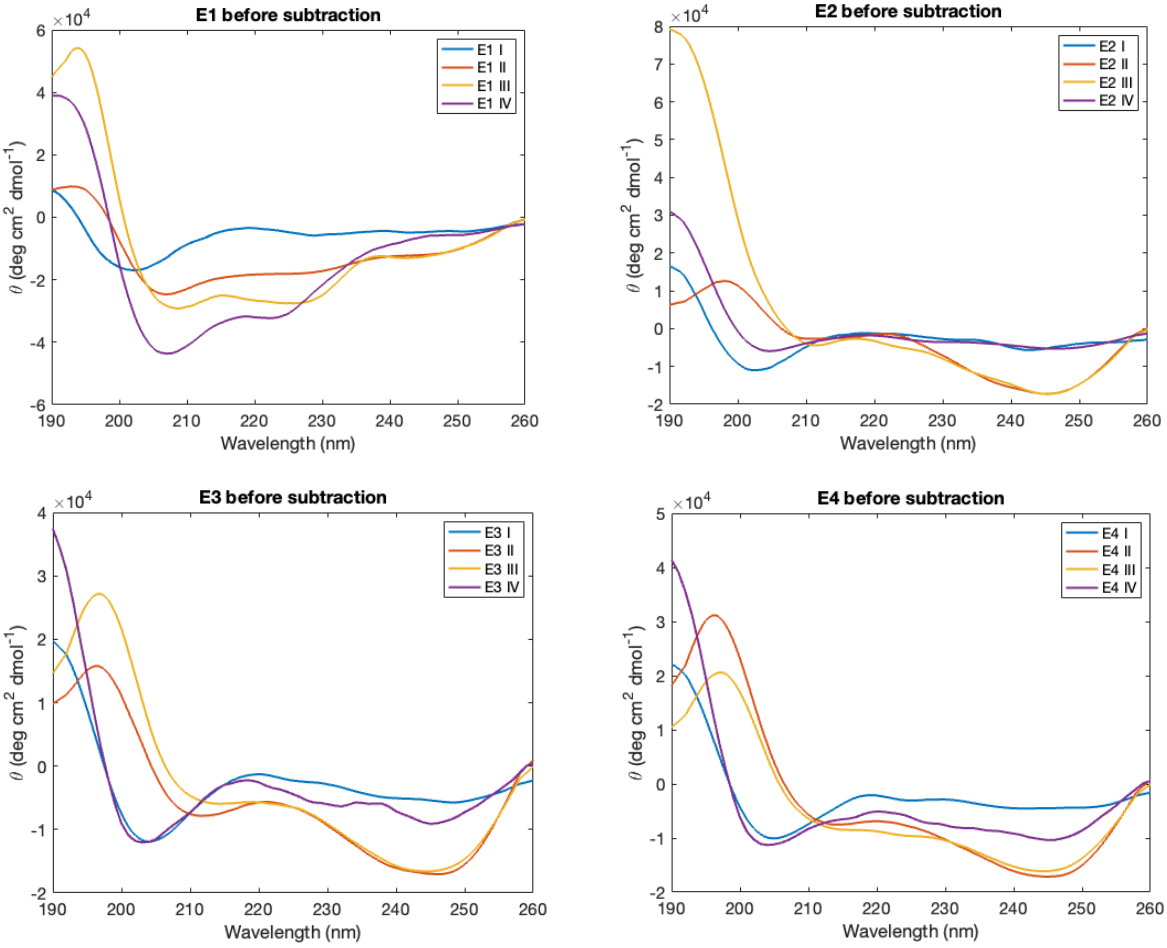

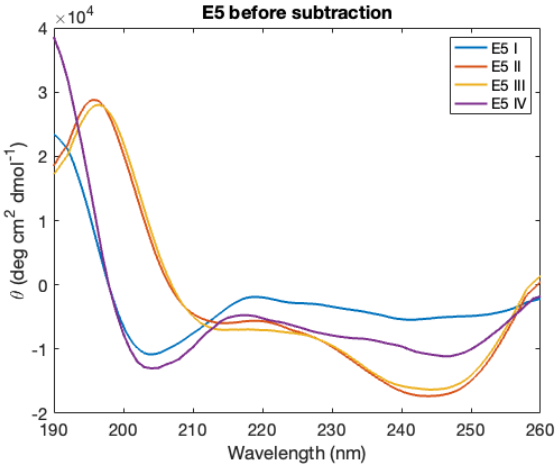
E5 before subtraction
×10^4
E5 I
E5 II
E5 III
E5 IV
θ (deg cm^2 dmol^-1)
Wavelength (nm)

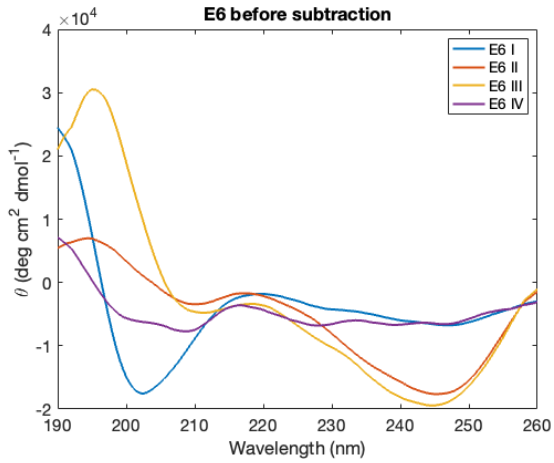
E6 before subtraction
×10^4
E6 I
E6 II
E6 III
E6 IV
θ (deg cm^2 dmol^-1)
Wavelength (nm)

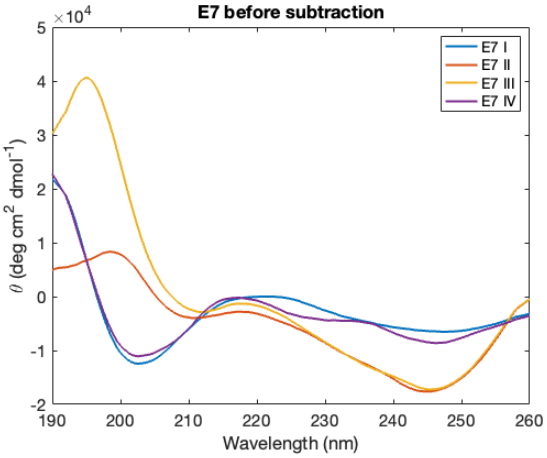
E7 before subtraction
×10^4
E7 I
E7 II
E7 III
E7 IV
θ (deg cm^2 dmol^-1)
Wavelength (nm)

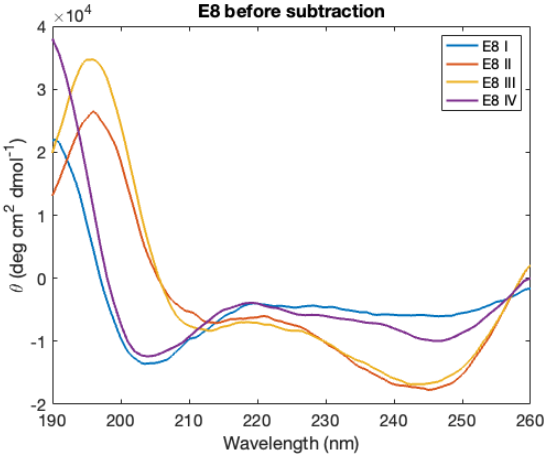
E8 before subtraction
×10^4
E8 I
E8 II
E8 III
E8 IV
θ (deg cm^2 dmol^-1)
Wavelength (nm)

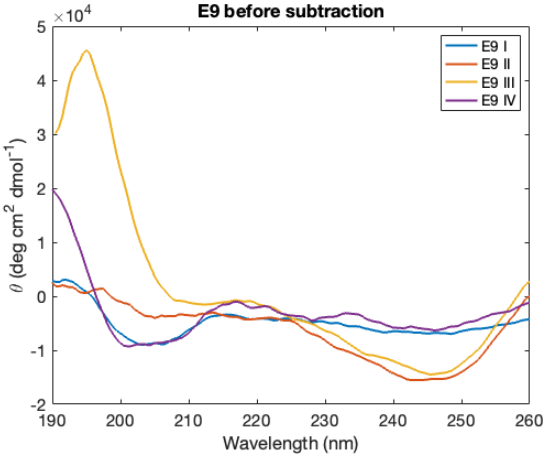
E9 before subtraction
×10^4
E9 I
E9 II
E9 III
E9 IV
θ (deg cm^2 dmol^-1)
Wavelength (nm)

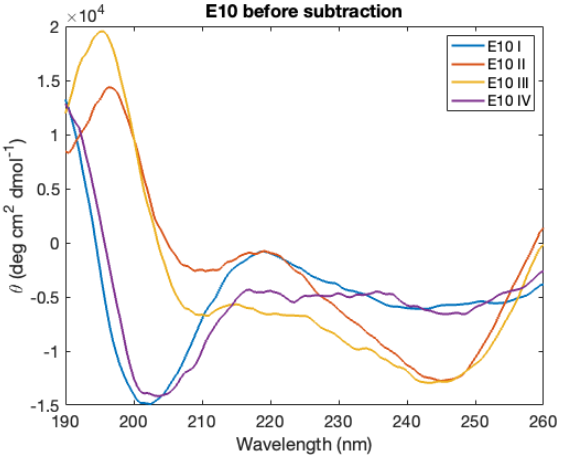
E10 before subtraction
×10^4
E10 I
E10 II
E10 III
E10 IV
θ (deg cm^2 dmol^-1)
Wavelength (nm)

Figure S9. CD spectrum of constructs E1-E10 before subtracting the DNA signal. Blue: single stranded DNA-peptide I; Orange: double stranded DNA-peptide II; Yellow: double stranded trimer III; Purple: singled stranded trimer IV.

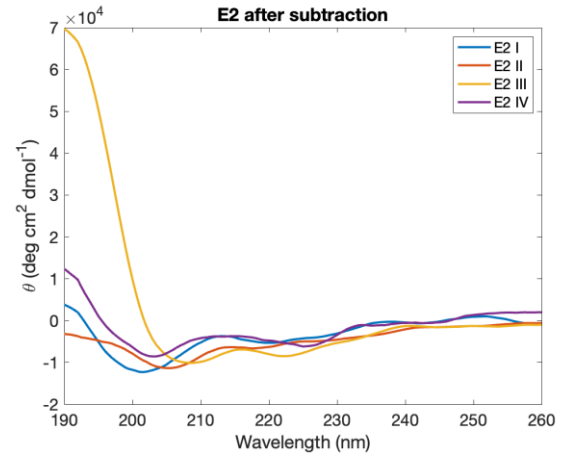

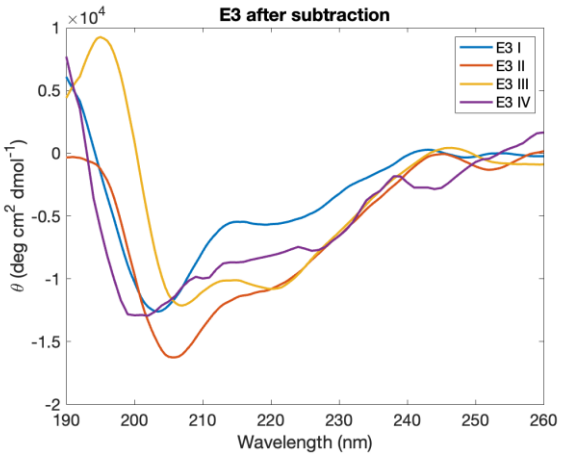

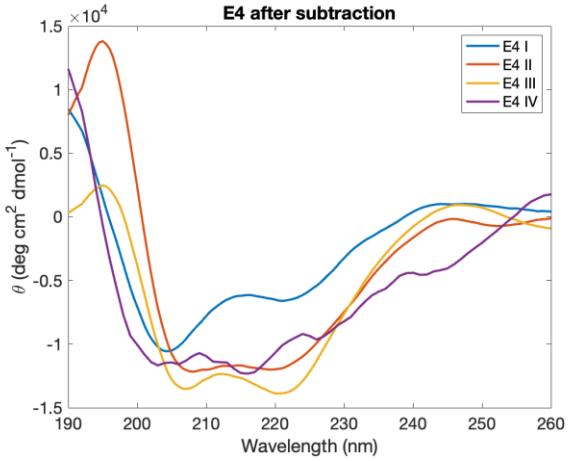

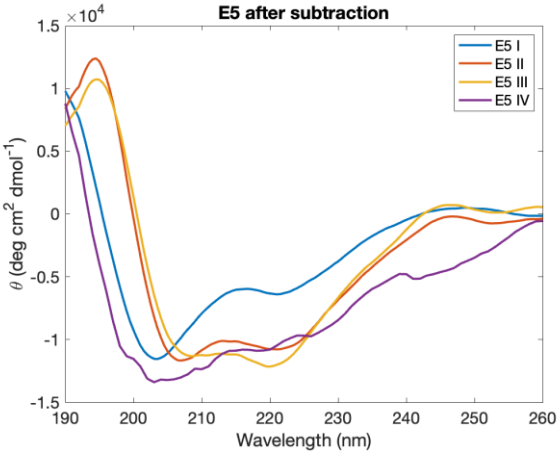

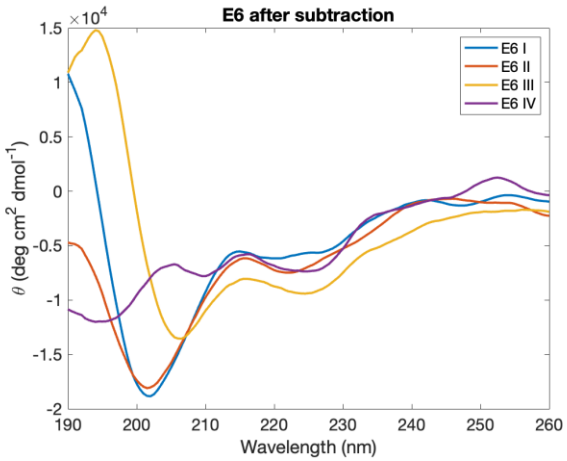

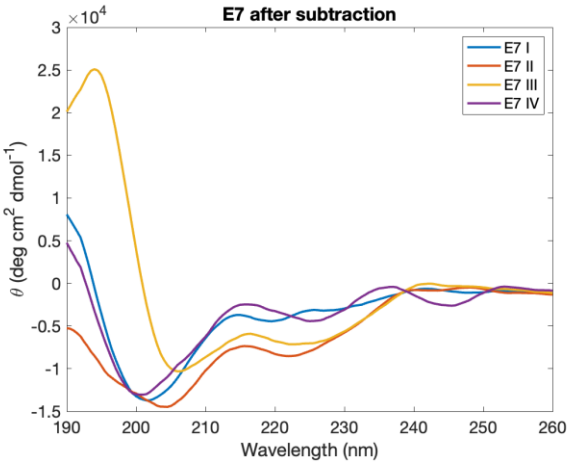

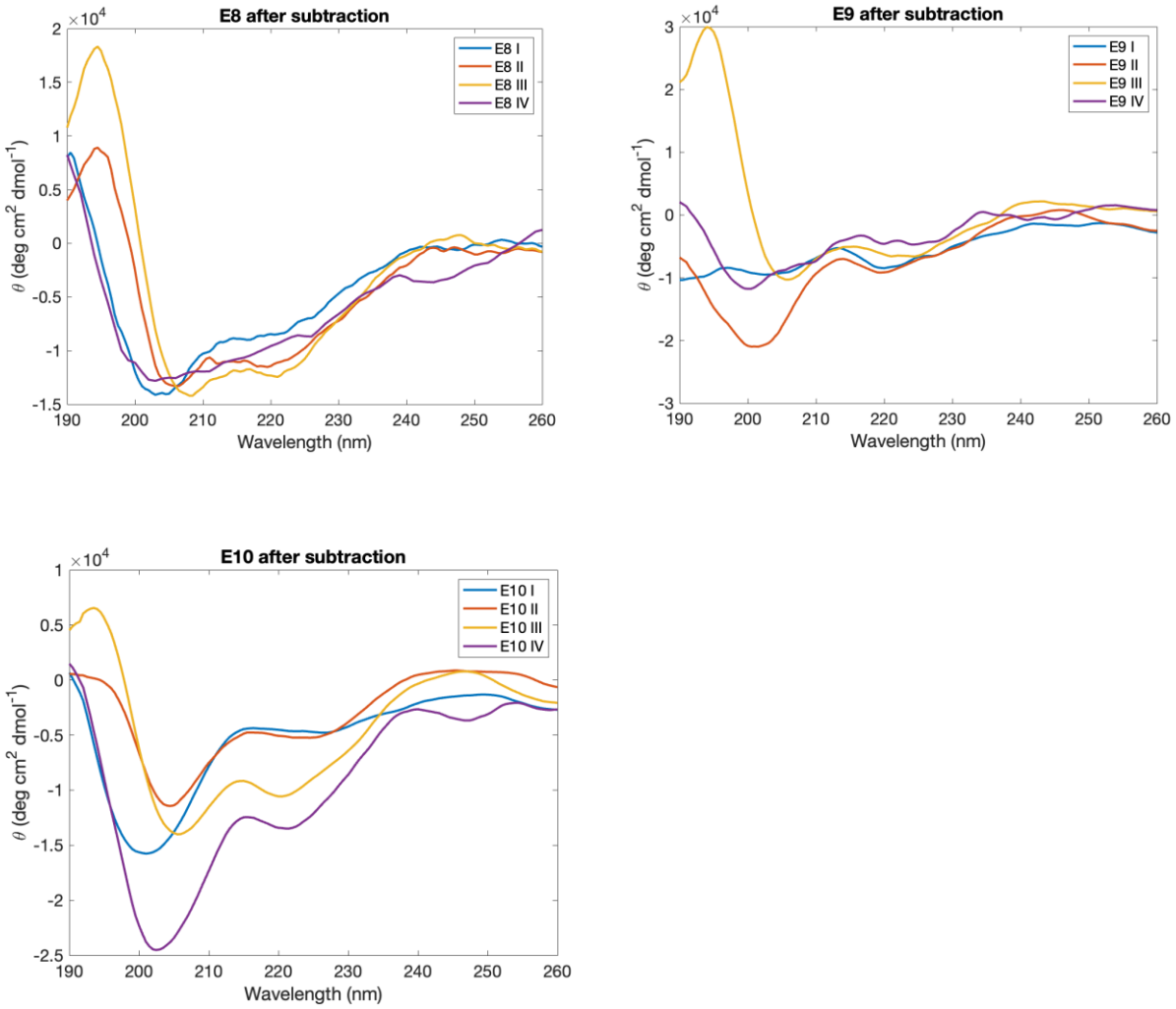

Figure S10. CD spectrum of constructs E2-E10 after subtracting the DNA signal. Blue: single stranded DNA-peptide I; Orange: double stranded DNA-peptide II; Yellow: double stranded trimer III; Purple: singled stranded trimer IV.

VIII. Secondary structure adjustment by DNA handle

1. Adjustment by scaffold central spacer

Single stranded DNA-peptide trimer E2 was mixed with 1 eq. of scaffold trimer with different central spacers (ST, ST1T, ST2T and ST4T) in 1x NaF. The mixture was annealed from 95 to 4 °C in 60 mins. 5% native PAGE gel was employed to check the assembly. The assembled nanostructures (1 μM) were analyzed by CD subsequently.

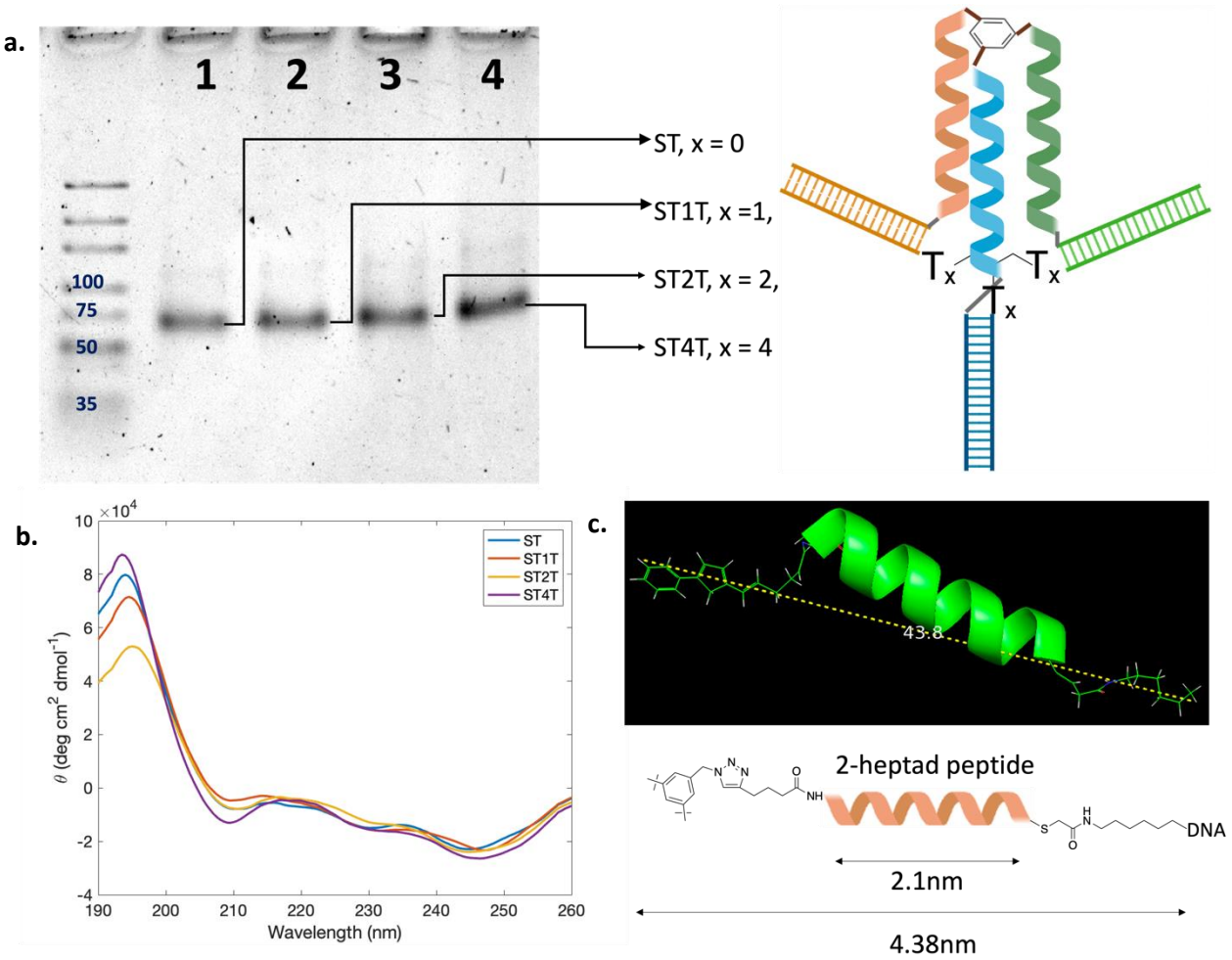

Figure S11. **a)** Native gel characterization of DNA-peptide trimer E2's assembly with ST (Lane 1), ST1T (Lane 2), ST2T (Lane 3) and ST4T (Lane 4). **b)** CD spectrum of assembled double stranded E2 trimer on different scaffolds before DNA background subtraction. **c)** Estimated length of stretched 2-hepatd peptide branch including the organic linkage in PyMol.

2. Control of peptide-peptide interactions by stretching DNA scaffolds

Singled stranded DNA-peptide trimer E5 was mixed with 1 eq. of 3WJ scaffolds (**Table S1**) in 1x NaF and the final concentration was 2 μM. The solution was then annealed from 95 to 4 °C in 6.5 hours. The assembly was checked by a 5% native gel (**Figure 7e**).

To control peptide secondary structure by facile DNA scaffolds, E4 trimer was annealed with equal amount of stretching strands with different spacers (**Table S1**) from 95 to 4 °C in 60 mins. The assembly was checked by native PAGE gel. High order structure was observed when E4 trimer assembled with stretching scaffolds with 25 bp spacer (sDTs25, sATs25), which is almost twice the length of the two peptide branches. Therefore, stretching scaffolds with 15 bp spacer (sDTs25, sATs25) was applied to E4 trimer for CD characterization.

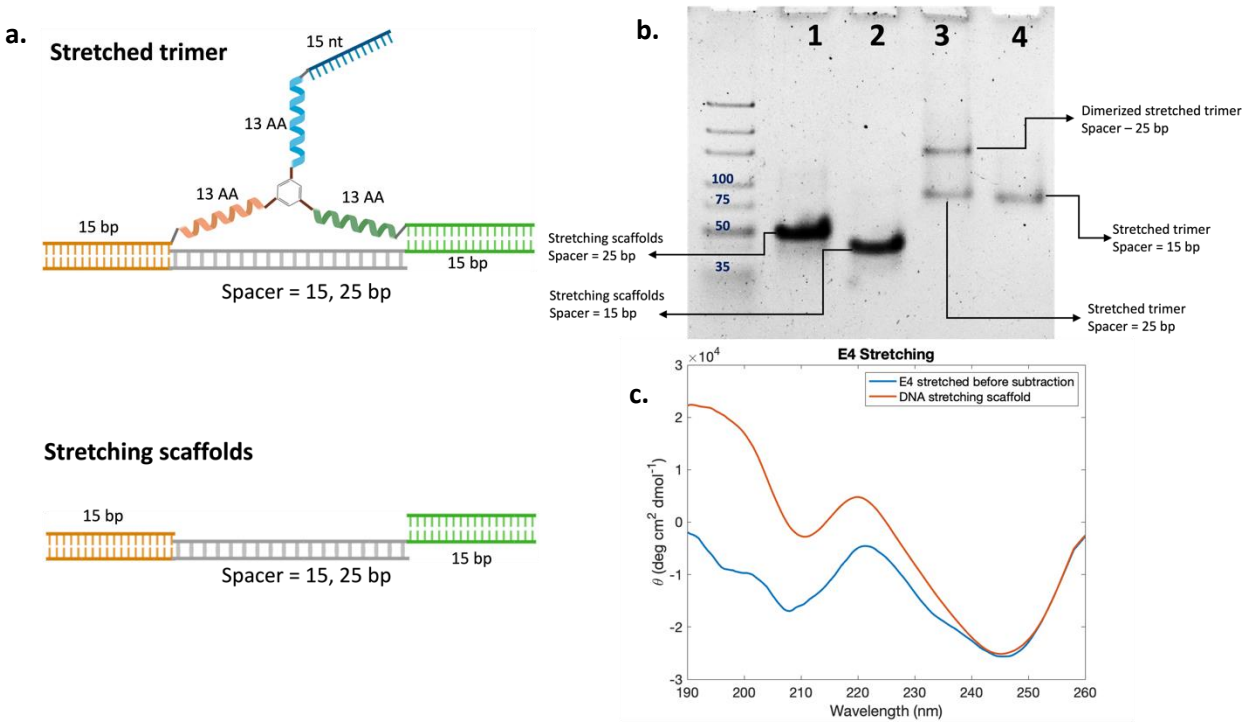

Figure S12. **a**) schematic representation of stretched trimer and stretching scaffolds. Stretched trimer (spacer = 15 bp) comprises of E4 trimer/A15/D15 = 1/1/1; stretched trimer (spacer = 25 bp) comprises of E4 trimer/A25/D25 = 1/1/1; stretching scaffolds (spacer = 15 bp) consists of A15/D15 = 1/1; stretching scaffolds (spacer = 25 bp) consists of A25/D25 = 1/1. **b**) 5% native PAGE gel of assembled stretched trimers and stretching scaffolds. **c)** CD characterization of stretching scaffolds (orange) and stretched trimer E4 before removing DNA signal (blue). 1.5 µM of each structure in 1x NaF was scanned.

IX. Thermal stability study

Samples were prepared as shown in **Table S2**. E5 III CD thermal stability experiments were carried out on Chirascan circular dichroism instrument. The other structures' CD thermal stability experiments were performed on JASCO J-810 spectropolarimeter.

1. Thermal stability study of E5 II (scaffolded) and E5 IV (stapled)

1a. Thermal denaturation of E5 II

In the case of E5 II, which only has external stabilizing force from DNA scaffolding, the structure's CD 222 nm signal exhibited a first increase with temperature going up to 40 °C (**Figure S13a**, stage 1), which indicates the dissociation of peptide-peptide interactions. As the temperature increased further, the CD signals at 222 nm indicated a second rise (**Figure S13a,** stage 2), consistent with α-helix melting.[1] Notably, past 54 °C, at which single-stranded DNA becomes the dominant species (**Figure S13c**, additional UV-260 nm thermal denaturation study for the DNA melting), the CD signal at 222 nm displayed a decreasing ellipticity (**Figure S13a,** stage 3), resembling the melting curve of short peptides with a random coil secondary structure.[2] This observation leads us to propose a three-step melting pathway for the scaffolded E5 II (**Figure S13d**). In stage 1, the coiled-coil dissociates and peptide-peptide interactions are denatured with a Tm of 35 °C. Stage II involves the melting of the DNA strands with a Tm of 48 °C and concomitant transition of the a-helix into a random coil structure, and stage 3 involves the complete denaturation of this random coil with a Tm of 59 °C. It is worth noting that the DNA Tm of

E5 II (scaffolded) is 14 °C lower than that of E5 III (scaffolded and stapled) because of the increased cooperativity from the organic stapling.

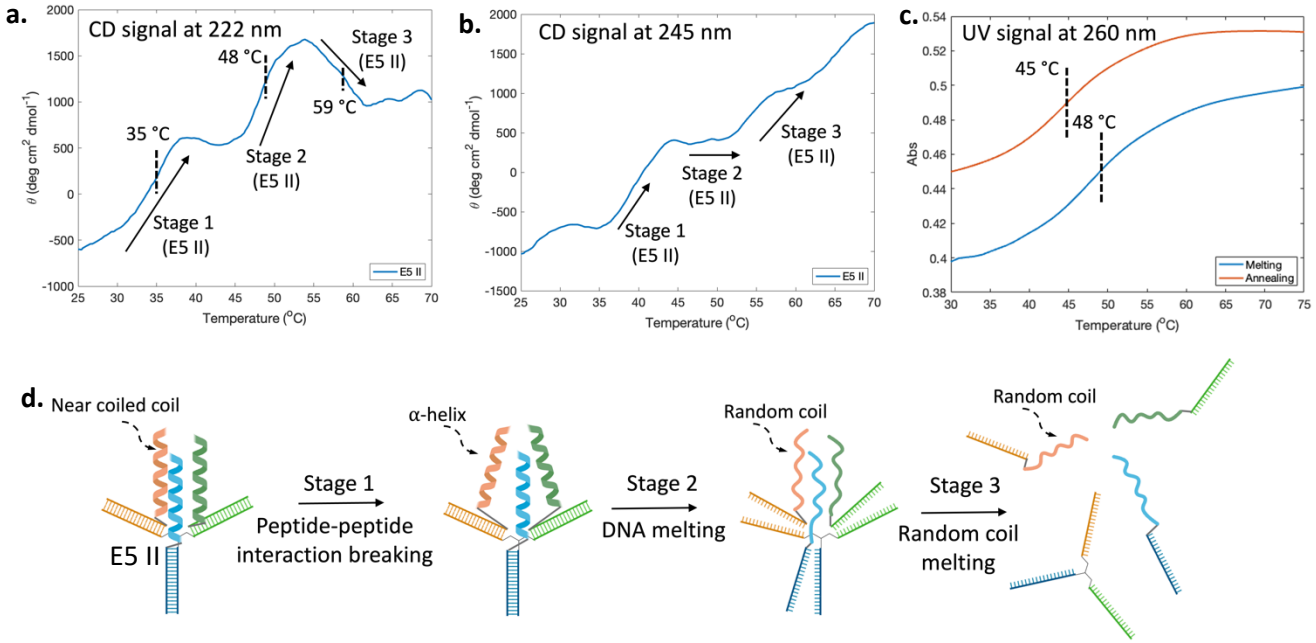

Figure S13. Thermal denaturation of E5 II. **a**) CD melting curve at 222 nm. **b**) CD melting curve at 245 nm. **c**) UV melting and annealing curves at 260 nm. **d**) Schematic representation of the melting pathway of E5 II.

1b. Thermal denaturation of E5 IV

In the case of E5 IV, where only organic stapling is present, the construct has a random coil peptide conformation at room temperature (**Figure S14a**). In this case, the single-stranded DNA melting curves shown by CD at 222 and 245 nm both exhibited fluctuating patterns (**Figure S14b & S14c**). It's therefore to be cautious in drawing quantitative conclusions about the CD thermal denaturation of E5 IV.

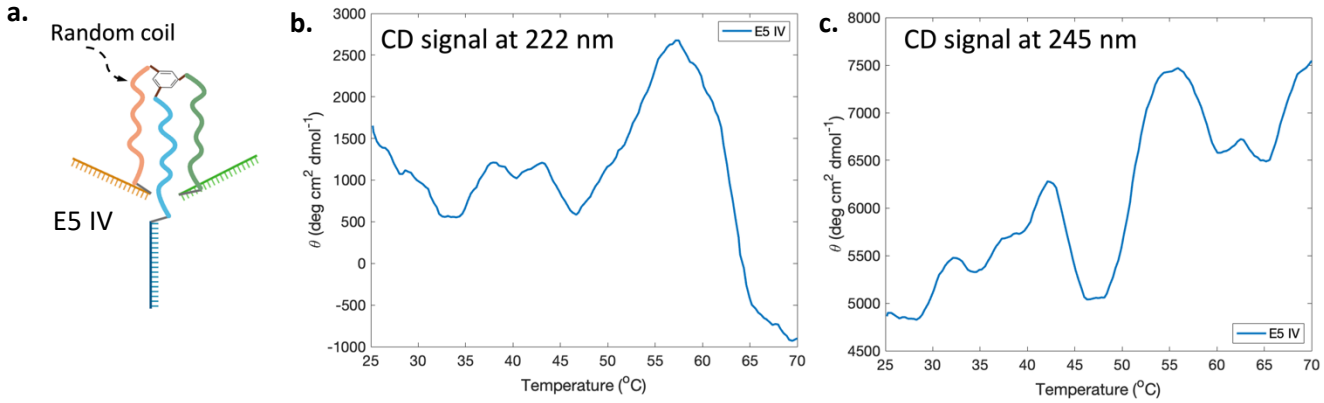

Figure S14. **a**) Schematic representation of E5 IV. **b**) CD melting curve at 222 nm. **c**) CD melting curve at 245 nm.

Based on the thermal denaturation study of E5 II, III (**Figure 8**) and IV, our findings suggest that DNA hybridization promotes both a-helix and peptide-peptide interactions. E5 II (scaffolded) demonstrates a near coiled-coil conformation at room temperature and exhibits a random coil melting pattern under conditions where DNA is denatured (**Figure S13a**). The introduction of covalent stapling impacts the Tm of the DNA portion, resulting in a 14 °C (**Figure S13c**, **Figure 8c**) increase observed between E5 II

(scaffolded) and E5 III (scaffolded and stapled). Furthermore, the covalent stapling strengthens interpeptide interactions, as evidenced by E5 III displaying a higher ratio of θ 222 nm / θ 208 nm at room temperature and a more pronounced coiled-coil melting pattern (**Figure 8b**) compared to E5 II (**Figure S13a**).

2. Thermal stability study of constructs with different peptide lengths

2a. Thermal denaturation of E8 III (3(2-heptad))

As shown in **Figure S15**, E8 III also showcased a two-stage melting pattern similar to E5 III (**Figure 8**) which contains the same length of peptides. The CD melting curves at 222 (**Figure S15a**) and 245 (**Figure S15b**) nm reveal synchronized patterns, with the first transition occurring at 36 °C and the second at around 60 °C. Given the similarity in results to those of E5 III, we consequently deduce that E8 III follows a comparable melting pathway (**Figure S15c**), where, with increasing temperature, peptide-peptide interactions first break, followed by DNA denaturation.

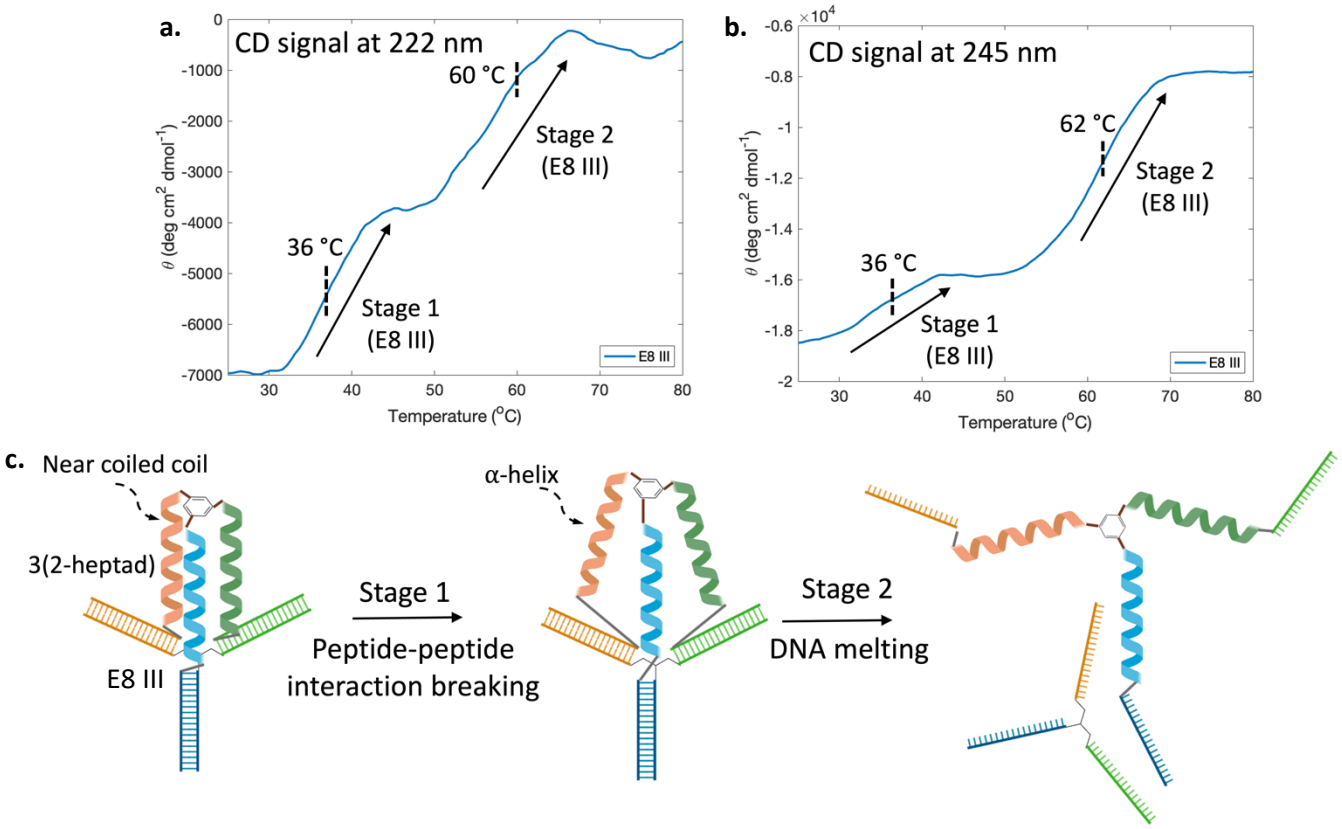

Figure S15. a) CD melting curve at 222 nm. **b**) CD melting curve at 245 nm. **c**) Schematic representation of the melting pathway of E8 III.

2b. Thermal denaturation of E1 III (3(3-heptad))

In the case of E1 III, the CD signals showcased three stages at 222 nm (**Figure S16a**) and 245 nm (**Figure S16b**). The first stage has a slow increase of ellipticity with increasing temperature up to 44 °C, indicating the breaking of interhelical peptide-peptide interactions. This is in line with the melting pattern of 3(2-heptad) constructs of E5 III (**Figure 8b**, stage 1) and E8 III (**Figure S15a**, stage 1). With the temperature continuing to rise, a stronger α-helix melting

pattern with a sharper ellipticity increase was observed from 44 to 54 °C in the second stage (**Figure S16a**, stage 2). Notably, the change in ellipticity of 222 nm is 6-fold greater than that observed in the 2-heptad constructs E5 II and E5 III. Considering that the difference between them is the peptide length, we attribute this transition to α-helix denaturation. The 3-heptad α helices continue to melt at stage 3, concurrently with DNA melting (**Figure S16b**, stage 3). We therefore propose a three-step melting pathway for E1 III (**Figure S16c**): initially, interpeptide interactions break with a Tm of 36 °C, followed by α-helix denaturation with a Tm of 47 °C, and DNA double strand denaturation happening at the last stage beyond 60 °C.

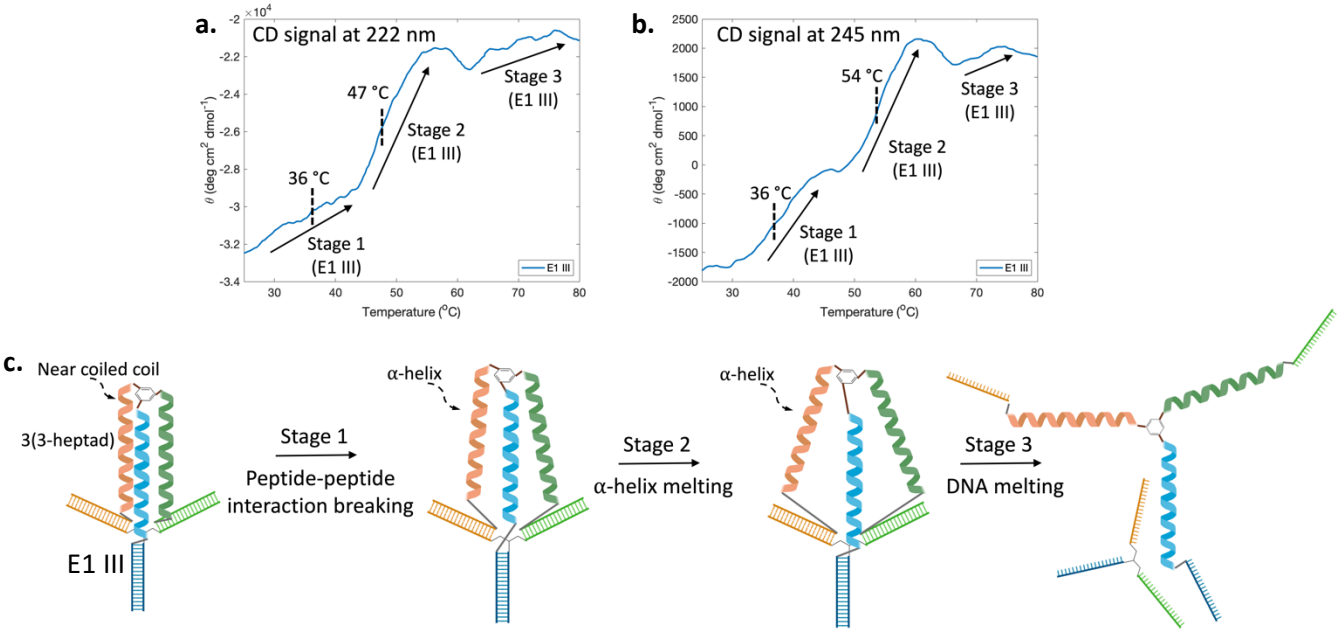

Figure S16. a) CD melting curve at 222 nm. **b**) CD melting curve at 245 nm. **c**) Schematic representation of the melting pathway of E1 III.

2c. Thermal denaturation of E10 III (2(2-heptad) + (3-heptad))

As for the length-mismatched construct E10 III, the peptide-peptide dissociation has a melting point of 36 °C (**Figure S17a**, stage 1), and the second α-helix melting has a melting point of 54 °C (**Figure S17a**, stage 2). Interestingly, after passing the DNA melting point of 60 °C (**Figure S17b**, stage 2), a random coil melting curve of decreasing CD signal at 222 nm emerged (**Figure S17a**, stage 3). This observation led us to hypothesize that due to the unconventional mismatch in peptide lengths, the dominant peptide conformation transformed into a random coil under denaturing DNA conditions (**Figure S17c**).

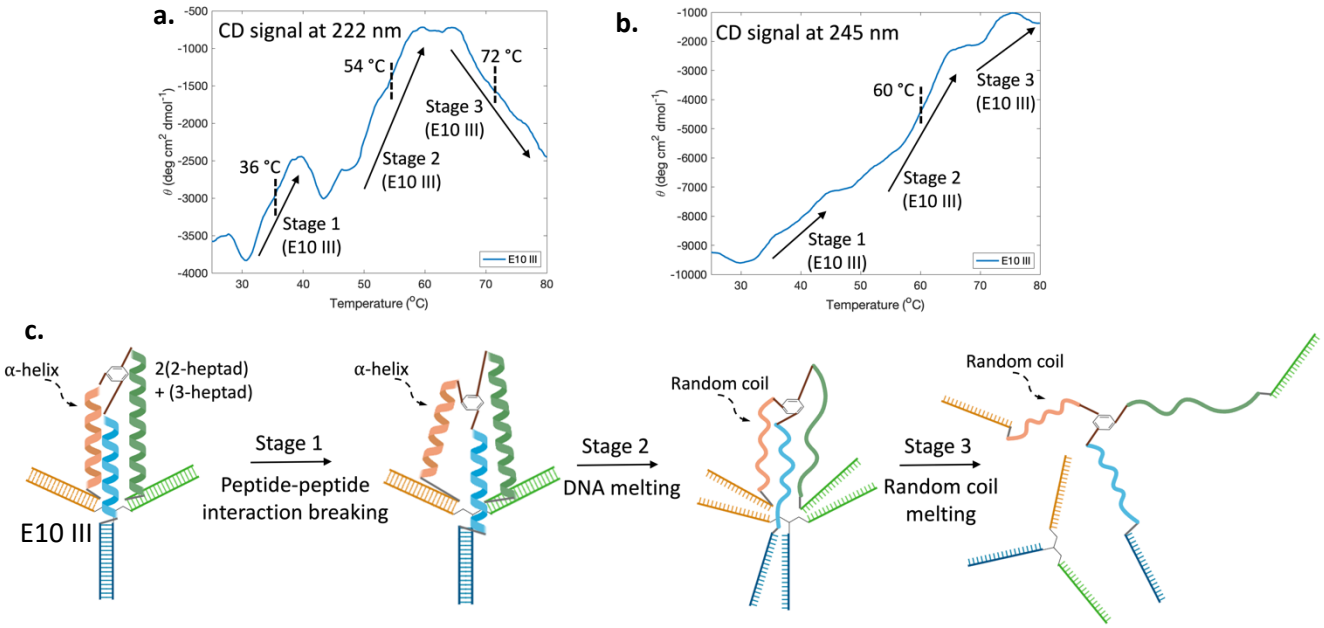

Figure S17. a) CD melting curve at 222 nm. **b**) CD melting curve at 245 nm. **c**) Schematic representation of the melting pathway of E10 III.

As a summary, we conclude that the double-stranded constructs with DNA scaffold have cooperative melting pathways from their DNA and peptide moieties as synchronized patterns were observed on CD-222 nm and CD-245 nm spectra. In addition, the DNA scaffolding contributes more to stabilizing the constructs as some structures (E5 II, E10 III) exhibited random coil patterns when the DNA is denatured. Moreover, the length of peptides can affect the overall stability as 3(3-heptad) construct E1 III exhibited different melting pathways from 3(2-heptad) constructs E5 III and E8 III.

Reference:

(1) Olamoyesan, A.; Ang, D.; Rodger, A. Circular dichroism for secondary structure determination of proteins with unfolded domains using a self-organising map algorithm SOMSpec. *RSC ADV.* **2021**, *11* (39), 23985-23991, 10.1039/D1RA02898G
(2) Gokce, I.; Woody, R. W.; Anderluh, G.; Lakey, J. H. Single Peptide Bonds Exhibit Poly(Pro)II ("Random Coil") Circular Dichroism Spectra. *J. Am. Chem. Soc.* **2005**, *127* (27), 9700-9701,